Editors' Suggestion

Thermal Hall conductivity in the strongest cuprate superconductor: Estimate of the mean free path in the trilayer cuprate $HgBa_2Ca_2Cu_3O_{8+\delta}$

Munkhtuguldur Altangerel,[1,2,3,*] Quentin Barthélemy,[1] Étienne Lefrançois,[1] Jordan Baglo,[1] Manel Mezidi,[1,3,4] Gaël Grissonnanche,[5] Ashvini Vallipuram,[1] Emma Campillo,[1] Anne Forget,[6] Dorothée Colson,[6] Ruixing Liang,[7,8] D. A. Bonn,[7,8] W. N. Hardy,[7,8] Cyril Proust,[2,3] and Louis Taillefer[1,3,8,†]

[1]*Institut Quantique, Département de Physique & RQMP, Université de Sherbrooke, Sherbrooke, Québec J1K 2R1, Canada*
[2]*LNCMI-EMFL, CNRS UPR3228, Université Grenoble Alpes, Université Toulouse, INSA-T, Grenoble and Toulouse, France*
[3]*Université de Sherbrooke–CNRS and IRL Frontières Quantiques, Sherbrooke, Québec, Canada*
[4]*Université Paris-cité, Laboratoire Matériaux et Phénomènes Quantiques, CNRS (UMR 7162), 75013 Paris, France*
[5]*Laboratoire des Solides Irradiés, CEA/DRF/lRAMIS, CNRS, École Polytechnique, Institut Polytechnique de Paris, 91128 Palaiseau, France*
[6]*Université Paris-Saclay, CEA, CNRS, SPEC, 91191 Gif-sur-Yvette, France*
[7]*Department of Physics and Astronomy, University of British Columbia, Vancouver, British Columbia, Canada*
[8]*Canadian Institute for Advanced Research, Toronto, Ontario M5G 1M1, Canada*

(Received 14 April 2025; revised 16 June 2025; accepted 18 June 2025; published 30 July 2025)

The thermal Hall conductivity of the trilayer cuprate $HgBa_2Ca_2Cu_3O_{8+\delta}$ (Hg1223)—the superconductor with the highest critical temperature T_c at ambient pressure—was measured at temperatures down to 2 K for three dopings in the underdoped regime ($p = 0.09, 0.10, 0.11$). By combining a previously introduced simple model and prior theoretical results, we derive a formula for the inverse mean free path, $1/\ell$, which allows us to estimate the mean free path of d-wave quasiparticles in Hg1223 below T_c. We find that $1/\ell$ grows as T^3, in agreement with the theoretical expectation for a clean d-wave superconductor. Measurements were also conducted on the single layer mercury-based cuprate $HgBa_2CuO_{6+\delta}$ (Hg1201), revealing that the mean free path in this compound is roughly half that of its three-layered counterpart at the same doping ($p = 0.10$). This observation is attributed to the protective role of the outer planes in Hg1223, which results in a more pristine inner plane. We also report data in an ultraclean crystal of $YBa_2Cu_3O_y$ (YBCO) with full oxygen content ($p = 0.18$), believed to be the cleanest of any cuprate, and find that ℓ is not longer than in Hg1223.

DOI: 10.1103/1gp5-h875

I. INTRODUCTION

The mean free path is a key property of electrons in metals. The most useful and simplest way to estimate the electronic mean free path ℓ_n is via the electrical resistivity ρ measured in the normal state, without superconductivity. In particular, the residual value at $T \to 0$, ρ_0, yields the elastic mean free path ℓ_{n0}, via the Drude formula

$$\rho_0 = \left(\frac{m^*}{ne^2}\right)\left(\frac{1}{\tau_{n0}}\right),$$

with $\ell_{n0} = v_F\tau_{n0}$, where v_F is the Fermi velocity, τ_{n0} is the scattering time at $T \to 0$, m^* is the effective mass, n is the density of charge carriers, and e is the electron charge. The mean free path ℓ_{n0} and the scattering rate $1/\tau_{n0}$ are quantitative measures of the scattering of electrons on defects in a sample in the normal state.

In d-wave superconductors, impurity scattering has a strong impact on superconducting properties because it easily breaks pairs. The strength of pair breaking is quantified by the ratio $\frac{\hbar/\tau_{n0}}{k_B T_c}$ (with $\hbar$ the reduced Planck constant $h/2\pi$, k_B the Boltzmann constant, and T_c the superconducting critical temperature). A ratio approaching 1 is expected to produce visible effects [1,2], such as a lower T_c, a lower superfluid density, and a deviation from the universal thermal conductivity at $T \to 0$ [3].

In cuprate superconductors, it has not been possible to estimate the electron mean free path in most samples because their robust superconductivity makes it difficult to measure ρ down to low temperatures. Measurements in high magnetic fields have provided some ρ_0 values in samples that have a relatively low upper critical field H_{c2}, typically at dopings near $p = 0.12$ or above $p \simeq 0.2$ [4]. For example, in overdoped $Tl_2Ba_2CuO_{6+\delta}$ (Tl2201) at $p = 0.29$ ($T_c = 15$ K, $H_{c2}(0) = 15$ T), $\rho_0 \simeq 6\ \mu\Omega$ cm [5], and in overdoped $Bi_2Sr_2CaCu_2O_{8+\delta}$ (Bi2212) at $p = 0.23$ ($T_c = 50$ K, $H_{c2}(0) = 50$ T), $\rho_0 \simeq 20\ \mu\Omega$ cm [6]. But in neither of these materials do we have any idea of ρ_0 in samples near optimal doping, since $H_{c2} \simeq 150$ T at such dopings [4].

In cuprates with a lower H_{c2}, resistivity measurements in pulsed fields up to 60–90 T can yield values for ρ in the $T \to 0$ limit across the full doping range. In overdoped $La_{2-x}Sr_xCuO_4$ (LSCO) with $p = 0.23$–0.24 [7,8] and $La_{1.6-x}Nd_{0.4}Sr_xCuO_4$ (Nd-LSCO) with $p = 0.24$ [9,10], this typically gives $\rho_0 \simeq 20\ \mu\Omega$ cm. However, in the underdoped regime, it is difficult to deduce a mean free path from the much

*Contact author: munkhtuguldur.altangerel@usherbrooke.ca
†Contact author: louis.taillefer@usherbrooke.ca

larger values of ρ in the $T \to 0$ limit, e.g., $\rho_0 \simeq 400\ \mu\Omega\,\mathrm{cm}$ in LSCO at $p \simeq 0.13$ [11], because we have little knowledge of the Fermi surface in that doping range, where pseudogap, spin glass phase, and charge order prevail and transform it profoundly [12–14].

There is clearly a need for another way to measure the electronic scattering rate and the mean free path in cuprates. Two decades ago, Zhang *et al.* [15] proposed an approach that has not been exploited much since. It is based on a measurement of the thermal Hall conductivity κ_{xy}, which can be performed below T_c in modest magnetic fields. The benefit of employing κ_{xy} as opposed to thermal conductivity κ_{xx} is that, in κ_{xx}, phonons contribute significantly alongside electrons, namely $\kappa_{xx} = \kappa_{qp} + \kappa_{ph}$. By contrast, in κ_{xy}, the contribution of phonons is negligible at low fields, allowing one to extract the electronic mean free path. A simple model then yields an estimate of ℓ_s, the mean free path of quasiparticles in the superconducting state. In ultraclean YBCO at $p = 0.18$, Zhang *et al.* found that $\ell_s \simeq 1\ \mu$m at $T \to 0$ and $H \to 0$ [15].

However, this model requires a knowledge of the specific heat of nodal quasiparticles. Concurrently, Vekhter *et al.* developed a theoretical formula for the specific heat of nodal quasiparticles [16]. By substituting their formula into the model proposed by Zhang *et al.* [15], one can derive an expression for the electronic mean free path that requires merely the thermal Hall conductivity κ_{xy}, the average distance between CuO_2 layers d, the Fermi wave vector k_F and the gap velocity v_Δ. v_Δ is the slope of the d-wave gap at the node, which can either be measured by angle-resolved photoemission spectroscopy (ARPES) [17,18] or accessed via the thermal conductivity in the $T \to 0$ limit [19–21].

In this article, we report measurements of κ_{xy} in three different cuprates: trilayer Hg1223 at $p = 0.09, 0.10$ and 0.11; single-layer Hg1201 at $p = 0.10$; bilayer YBCO at $p = 0.18$. In the superconducting state, we find that $1/\ell_s$ displays a T^3 dependence, as expected theoretically for a clean d-wave superconductor [22–25]. We obtain the residual value of the mean free path, ℓ_{s0} at $T \to 0$, for each sample, allowing us to compare amongst cuprates. We find that our Hg1223 samples are as clean as the cleanest YBCO samples.

II. METHODS

A. Samples

High-quality single crystals of Hg1223 with dopings $p = 0.09$, $p = 0.10$, and $p = 0.11$ were grown using the self-flux technique [26]. Doping levels were determined using the empirical relationship [27]

$$1 - T_c/T_{c,\max} = 82.6(p - 0.16)^2,$$

where T_c denotes the onset of the superconducting transition and $T_{c,\max}$, the critical temperature of optimally doped Hg1223, is 135 K. The $p = 0.09$ sample had $T_c = 78$ K, the $p = 0.10$ sample had $T_c = 95$ K, and the $p = 0.11$ sample had $T_c = 112$ K.

A single high-purity crystal of underdoped Hg1201 ($p = 0.10$, $T_c = 76$ K) was measured, prepared as described in [28,29]. The doping level was determined based on the $T_c(p)$ relationship for Hg1201 established in [30].

TABLE I. Properties of the measured samples, including the superconducting transition temperature T_c, hole doping level p, interplane distance d, and mean free path ℓ_{s0} at $T \to 0$ and $B = 0.5$ T. The error bars on ℓ_{s0} include uncertainty from approximation, fitting and geometrical factors. Here, d represents the interplane distance, with $d = 5.3$ Å or $d = 16$ Å for Hg1223, depending on whether it is calculated as $c/3$ or c, respectively. The ℓ_{s0} values for Hg1223 correspond to the case $d = c/3$ (with all planes considered equivalent).

Compound	T_c (K)	p	d (Å)	ℓ_{s0} (Å)
Hg1223	78	0.09	5.3 or 16	1180 ± 170
Hg1223	95	0.10	5.3 or 16	1590 ± 230
Hg1223	112	0.11	5.3 or 16	2760 ± 390
Hg1201	76	0.10	9.5	1040 ± 150
YBCO	90.5	0.18	5.8	3530 ± 500

Single crystals of YBCO with $p = 0.18$ were grown by flux growth, as described in [31]. Our sample was a single detwinned crystal with an oxygen content $y = 6.998$, corresponding to $T_c = 90.5$ K.

All samples were prepared as rectangular platelets, with gold sputtered contacts and subsequent silver paint applied for electrical measurements. The typical dimensions of the samples are 300–1000 × 300 μm, with a thickness of ∼100 μm.

The interplane distance d represents the average separation between CuO_2 planes. For Hg1201, $d = 9.5$ Å, corresponding to the distance between CuO_2 planes. For YBCO, $d = 5.8$ Å, the average separation between CuO_2 planes in the unit cell. In the case of Hg1223, there are two possible ways to define d: $d = \frac{c}{3}$ if we treat all three planes as equivalent, where $c = 15.86$ Å, or $d = c$ if we consider only the distance between the inner planes (see discussion below). The values of T_c and d are given in Table I.

B. Thermal transport measurement

The measurement of thermal conductivity κ_{xx} involves applying a heat power $\dot{Q}_x$ along the x axis of the sample, causing a longitudinal temperature difference $\Delta T_x = T^+ - T^-$. Equation (1) provides the expression for κ_{xx}:

$$\kappa_{xx} = \frac{\dot{Q}_x}{\Delta T_x}\left(\frac{L}{wt}\right), \tag{1}$$

where w is the width of the sample, t is its thickness, and L is the distance between T^+ and T^-. When a magnetic field is applied along the z axis, a transverse temperature difference ΔT_y can develop along the y axis. Equation (2) defines the thermal Hall conductivity κ_{xy}:

$$\kappa_{xy} = -\kappa_{yy}\frac{\Delta T_y}{\Delta T_x}\frac{L}{w} \tag{2}$$

with κ_{yy} representing the thermal conductivity in the y direction. This expression is an approximation that holds when $\kappa_{xy}/\kappa_{xx} \ll 1$, a condition that is satisfied for all our measurements. In a tetragonal system such as Hg1223 and Hg1201, κ_{yy} is equal to κ_{xx}. The temperature differences ΔT_y and ΔT_x were measured using type E thermocouples (chromel constantan) in a steady-state method in a fixed magnetic field B. This

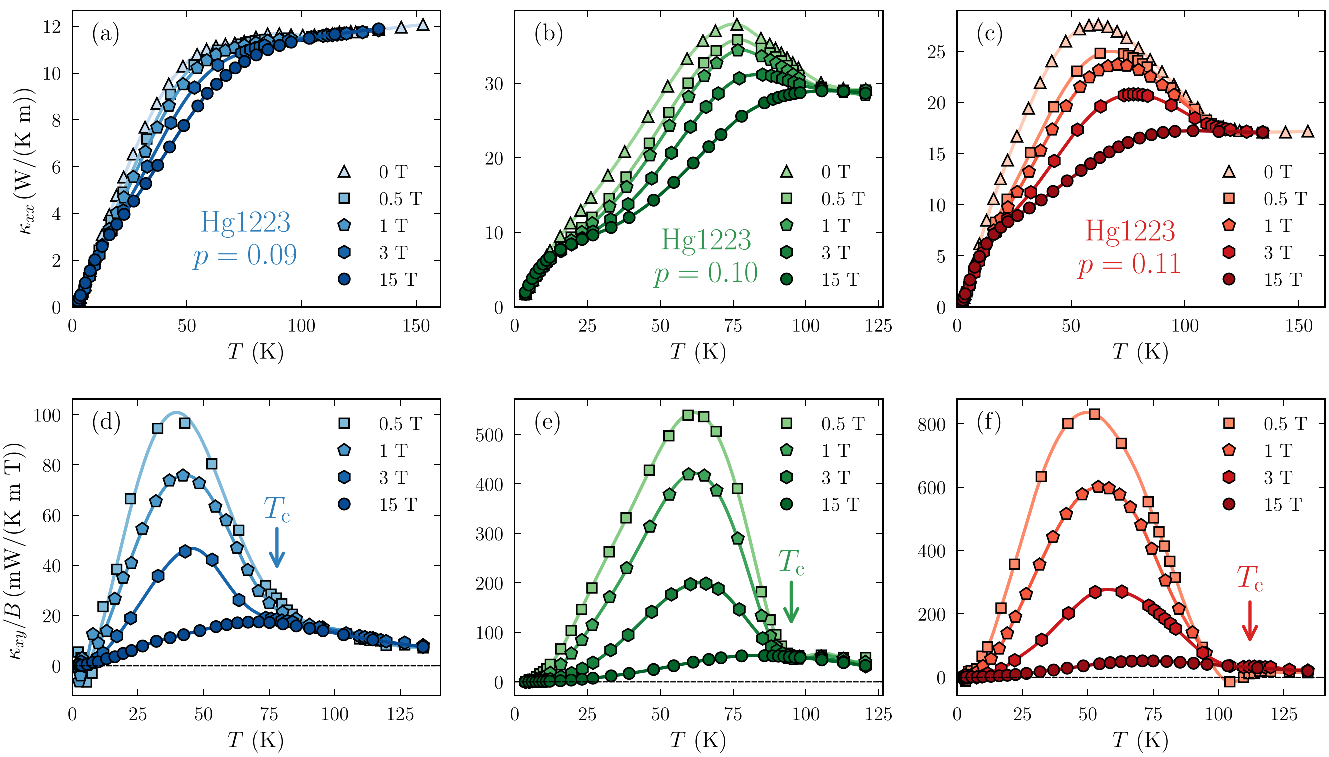

FIG. 1. Thermal conductivity of Hg1223. Longitudinal thermal conductivity κ_{xx} and thermal Hall conductivity normalized by field κ_{xy}/B for Hg1223 ($p = 0.09, 0.10, 0.11$) as a function of temperature T in magnetic fields of 0 T (triangles), 0.5 T (squares), 1 T (pentagons), 3 T (hexagons), and 15 T (circles), with darker shades indicating higher fields. Lines serve as guides to the eye, while markers represent the data points. Panels (a)–(c) show κ_{xx}: (a) Hg1223 $p = 0.09$ (blue); (b) Hg1223 $p = 0.10$ (green); (c) Hg1223 $p = 0.11$ (red). Panels (d)–(f) show κ_{xy}/B. The arrows indicate the location of the superconducting transition.

choice was based on the weak-field dependence of type-E thermocouples within the explored temperature and magnetic-field range, offering a better sensitivity than resistive Cernox sensors at high temperatures.

To measure κ_{xy} accurately, any contamination from thermal conductivity κ_{xx} due to a slight misalignment of the two opposite transverse contacts is eliminated by field antisymmetrization. This involves calculating $\Delta T_y^{\rm as}(T, B) = [\Delta T_y(T, B) - \Delta T_y(T, -B)]/2$, where $\Delta T_y^{\rm as}(T, B)$ represents the antisymmetrized $\Delta T_y(T, B)$. The heat current along the x axis is generated by a strain gauge heater attached to one end of the sample, and the other end connected to a copper block using silver paint, serving as a heat sink.

For YBCO, which is orthorhombic, κ_{yy} was measured in a separate sample with the heat current applied along the y direction (corresponding to the crystallographic b axis) [32]. In this case, the thermal Hall conductivity κ_{xy} was calculated using the measured κ_{yy} in combination with the method described above.

For a more comprehensive discussion of the thermal transport measurement technique, the reader is referred to [32–37], where the measurements were carried out using the same experimental methodology.

III. RESULTS

In Fig. 1, the thermal conductivity κ_{xx} and the thermal Hall conductivity divided by the magnetic field κ_{xy}/B are presented for three Hg1223 samples at dopings $p = 0.09$, 0.10, and 0.11 for various magnetic fields ($B = 0$, 0.5, 1, 3, and 15 T) from 3 K to 140 K.

The thermal conductivity κ_{xx} exhibits a prominent peak upon entering the superconducting state at low fields in the $p = 0.10$ and $p = 0.11$ samples (top panels). This peak results from a sharp reduction in inelastic electron-electron scattering as electrons condense into Cooper pairs, leading to a substantial increase in the electronic mean free path [38]. In contrast, the $p = 0.09$ sample shows a significantly reduced peak.

When elastic scattering dominates over inelastic scattering, a peak in thermal conductivity is not expected in the superconducting state of a d-wave superconductor. The diminished peak in the $p = 0.09$ sample [Fig. 1(a)] points to a larger ratio of elastic to inelastic scattering. This is in part due to the lower T_c, making inelastic scattering at the transition weaker than in the samples with higher T_c. But it may also reflect a higher level of disorder.

In the lower panels of Fig. 1, we see that the magnitude of the peak in κ_{xy}/B differs between the samples despite similar doping levels, where comparable electron densities are expected. This difference likely arises from variations in disorder, which we will quantify in the Discussion section. The $p = 0.11$ sample has the highest peak value, namely $\kappa_{xy}/B \approx 800$ mW/(K m T) at $B = 0.5$ T, while the $p = 0.09$ sample shows a peak value of $\kappa_{xy}/B \approx 100$ mW/(K m T).

Figure 2 presents the thermal conductivity κ_{xx} and the thermal Hall conductivity divided by the magnetic field κ_{xy}/B for single-layer Hg1201 and bilayer YBCO at magnetic fields $B = 0.5$ and 3 T. For Hg1201, the same fields as used for

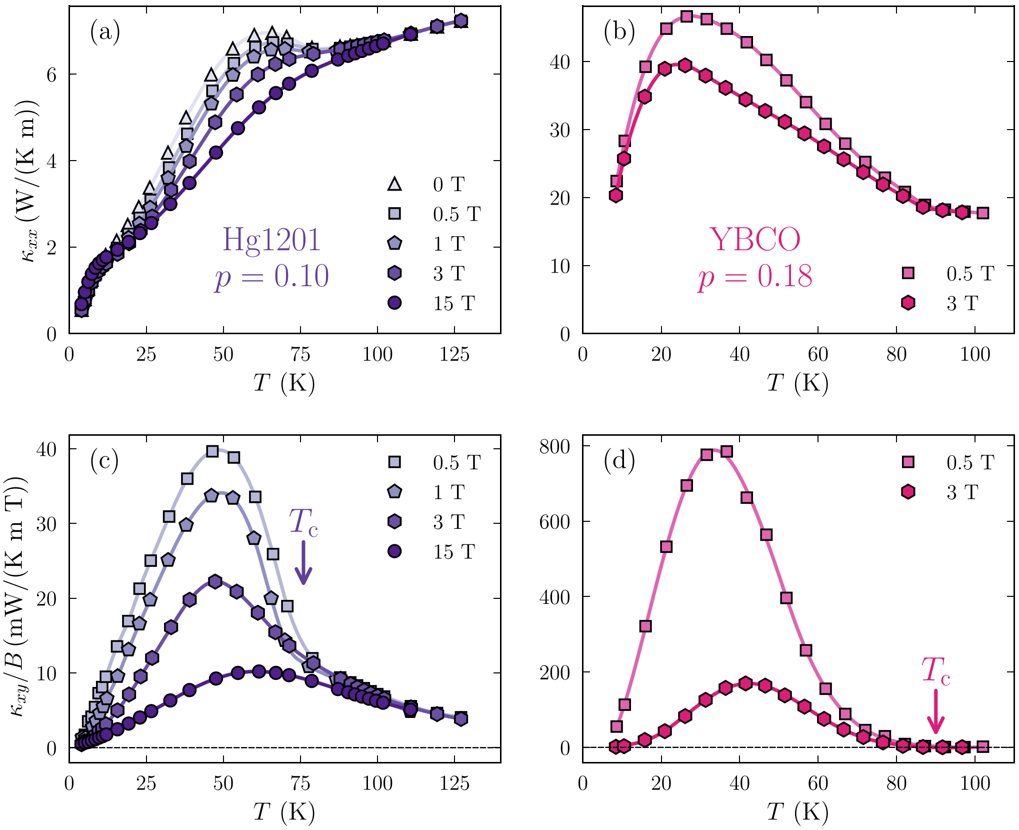

FIG. 2. Thermal conductivities in Hg1201 and YBCO. Longitudinal thermal conductivity κ_{xx} and transverse thermal conductivity normalized by field κ_{xy}/B for Hg1201 ($p = 0.10$) and YBCO ($p = 0.18$) as a function of temperature T. For Hg1201, data are shown for magnetic fields of 0 T (triangles), 0.5 T (squares), 1 T (pentagons), 3 T (hexagons), and 15 T (circles), with darker shades indicating higher fields. For YBCO, data are presented for 0.5 T (squares) and 3 T (hexagons). Lines serve as guides to the eye, while markers represent the data points. Panels (a)–(b) show κ_{xx}: (a) Hg1201 ($p = 0.10$, purple); (b) YBCO ($p = 0.18$, pink). Panels (c)–(d) show κ_{xy}/B. The arrows indicate the location of the superconducting transition.

Hg1223 are included. The peak value of κ_{xy}/B in Hg1201 is notably low compared to Hg1223, around 40 mW/(K m T). This reduced conductivity is attributed to the higher disorder in Hg1201, as it lacks the multilayer structure that provides protection of the inner layer from impurities. In contrast, YBCO—known to be the cleanest among cuprates—exhibits a κ_{xy}/B signal comparable to Hg1223 at $p = 0.11$, approximately 800 mW/(K m T). This similar magnitude strongly suggests that Hg1223 is also exceptionally clean, with its inner plane protected by the outer planes, minimizing disorder.

Figure 3 shows κ_{xy}/B measured in the lowest field for our three Hg1223 samples. These data are used to extract the mean free path of nodal quasiparticles, in the next section.

IV. DISCUSSION

The advantage of using thermal transport to estimate the mean free path of electrons is that it can be measured in the superconducting state, at low fields. However, to use the thermal conductivity κ_{xx} is challenging because phonons also make a large contribution to κ_{xx}. This is why we turn to the thermal Hall conductivity κ_{xy}, which is typically dominated by electrons at low fields.

Before turning to the interpretation of the mean free path data, we first address the possible contribution of phonons to the sizable thermal Hall response in our samples. Since 2020, it has been established that phonons can generate a sizable

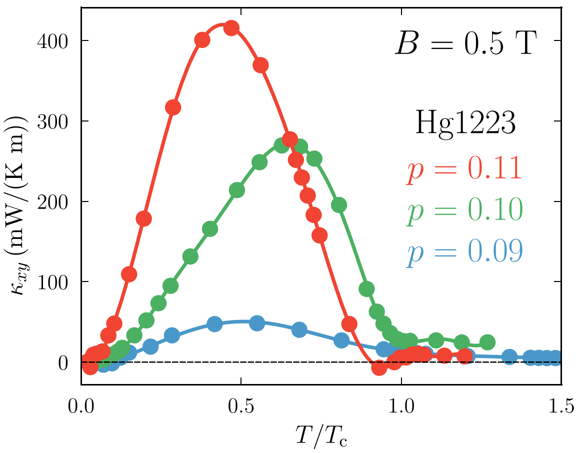

FIG. 3. Thermal Hall conductivity κ_{xy} as a function of reduced temperature T/T_c for Hg1223 at $B = 0.5$ T: $p = 0.09$ (blue), $p = 0.10$ (green), and $p = 0.11$ (red). Lines serve as guides to the eye, while markers represent the data points. These data are used to extract the mean free path ℓ_s in Hg1223.

thermal Hall response in both hole- and electron-doped cuprates [33,37,39–41]. In all such materials studied to date—including LSCO, Eu-LSCO, Nd-LSCO, Bi2201, NCCO, and PCCO—the phonon thermal Hall conductivity is consistently negative in sign.

Assuming the same sign applies to Hg1223, Hg1201, and YBCO, the fact that we observe a positive κ_{xy} in all three compounds strongly suggests that the signal is electronic in origin. Furthermore, the magnitude of the thermal Hall conductivity in our measurements far exceeds typical phonon values. For instance, in LSCO ($x = 0.06$) at 50 K and 1 T, the phonon Hall conductivity is about $\kappa_{xy}/B \sim -2$ mW/(K m T) [42], whereas the signal in Hg1223 (Fig. 1) and YBCO [Fig. 2(d)] is roughly two orders of magnitude larger, and about one order of magnitude larger in Hg1201 [Fig. 2(c)]. This shows that the phonon contribution to κ_{xy} is negligible in all samples studied here, at least at low fields.

A. Model

The model from [15] is first presented to derive the thermal mean free path from κ_{xy}, and then extended for a broader application to any d-wave superconductor using the theoretical framework from [16]. In the weak magnetic field regime ($\omega_c\tau \ll 1$), where ω_c is the cyclotron frequency, the Boltzmann transport formalism is valid. For this analysis, the thermal mean free path is extracted at $B = 0.5$ T. This field value represents a compromise: it is high enough to yield a good signal-to-noise ratio while keeping $\omega_c\tau \ll 1$, ensuring the applicability of the theoretical framework. Moreover, the assumption $\omega_c\tau \ll 1$ will be verified later to ensure the self-consistency of this approach. Measuring κ_{xy} at low fields minimizes the phonon contribution, making the electronic response the dominant factor (see above).

The essence of this model is the assumption that, in the weak-field regime, the thermal Hall conductivity κ_{xy} is related to the longitudinal thermal conductivity of the quasiparticles κ_{qp} through the following relation:

$$\kappa_{xy}/\kappa_{qp} = \eta\omega_c\tau = \eta\frac{\ell}{k_F\ell_B^2}, \tag{3}$$

where $\ell_B = \sqrt{\hbar/eB}$ is the magnetic length. The parameter η accounts for the anisotropy of the scattering path length across the Fermi surface [15]. However, due to limited knowledge of η in the studied samples, we assume $\eta = 1$ for all three cuprates under investigation: Hg1223, YBCO, and Hg1201.

Following Zhang *et al.* [15] we define the thermal conductivity of nodal quasiparticles in the superconducting state:

$$\kappa_{qp} = c_{qp}v_F\ell/4, \tag{4}$$

where v_F is the normal-state Fermi velocity in the nodal direction and c_{qp} is the specific heat of the nodal quasiparticles, which varies quadratically with temperature:

$$c_{qp} = \alpha_c T^2. \tag{5}$$

The prefactor α_c was measured experimentally in YBCO ($p \simeq 0.16$) as $\alpha_c = 0.064$ mJ/K^3 mol [43]. Combining the expressions for κ_{xy}/κ_{qp} and κ_{qp} leads to the following equation for the mean free path ℓ_s, derived in [15]:

$$\ell_s = 2\ell_B\sqrt{\frac{\kappa_{xy}k_F}{c_{qp}v_F\eta}}. \tag{6}$$

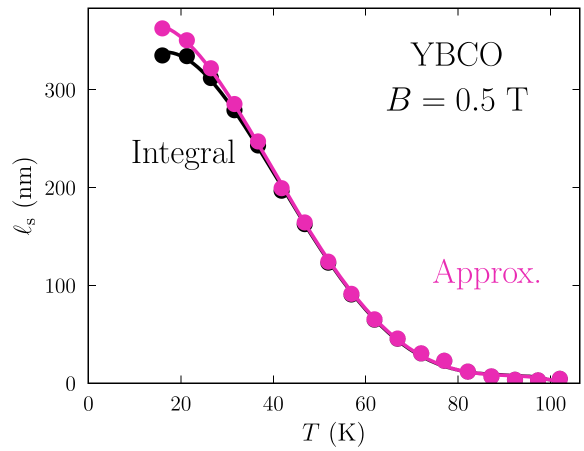

FIG. 4. Mean free path ℓ_s as a function of temperature T in YBCO ($p = 0.18$), calculated using two different forms of the quasiparticle specific heat c_{qp}. The black markers represent ℓ_s extracted using the integral form of c_{qp}, given in Eq. (63) of [16], while the pink markers correspond to ℓ_s obtained with the approximate expression, Eq. (7). Lines are a guide to the eye. The two methods show excellent agreement for $T > 30$ K, with deviations remaining below 10% at lower temperatures. The uncertainty associated with this deviation is included in the error bar on the mean free path values we quote in the text and in Table I.

In addition to k_F and v_F, this formula requires knowledge of the specific heat coefficient α_c, which is not often accessible. To address the practical limitations in accessing this parameter, we introduce an alternative formulation for ℓ_s that depends instead on the gap velocity v_Δ. This is achieved using the theoretical expression for c_{qp} of d-wave superconductors [16]:

$$c_{qp} = \frac{18k_B^3\zeta(3)}{\hbar^2 d\pi v_F v_\Delta}T^2, \tag{7}$$

where ζ is the Riemann zeta function. A comparison between theoretical and experimental values of α_c in YBCO shows excellent agreement–the theoretical estimate is only 1.2 times the measured value (using $v_F = 2.5 \times 10^5$ m/s and $v_\Delta = 1.5 \times 10^4$ m/s [44]). This supports the use of the theoretical form for analyzing Hg1223 and Hg1201, where experimental values of α_c are not available.

Equation (7) is valid under the condition $E_H \ll T$, where $E_H \sim 30\sqrt{B}$ K/T$^{1/2}$ represents the Doppler shift energy scale in d-wave superconductors [16]. For $B = 0.5$ T, $E_H \simeq 21$ K, making Eq. (7) applicable above this temperature.

To validate the T^2 approximation for the quasiparticle specific heat [Eq. (7)], we compare in Fig. 4 the mean free path ℓ_s obtained using two forms of α_c: the full integral expression from Eq. (63) of Ref. [16], valid across all temperatures and fields, and the simplified form from Eq. (7) used in this work. As expected, both approaches yield nearly identical results at temperatures well above 21 K. At lower temperatures, where the approximation breaks down, the deviation in ℓ_s is less than 10%; the associated uncertainty is included in the error bars of the quoted values (see Table I).

Substituting Eq. (7) into Eq. (6) yields

$$\ell_s = \ell_B \sqrt{\frac{2\pi\hbar^2}{9\zeta(3)k_B^3}} \sqrt{\frac{v_\Delta k_F d\kappa_{xy}}{\eta T^2}}. \quad (8)$$

Note that this expression is broadly applicable to superconductors for which a Boltzmann transport approach is deemed valid, including multiband and three-dimensional cases, provided the Fermi surface and gap velocity are known.

B. Analysis

From Eq. (8), what we need is the value of k_F and v_Δ, in the nodal direction (We assume $\eta = 1$.). This knowledge does not exist for all materials and all dopings. Detailed ARPES studies of the bilayer cuprate Bi2212 reveal that v_Δ is constant and equal to 1.5×10^4 m/s between $p = 0.08$ and $p = 0.20$ [18]. It is well known that the nodal wave vector varies only slightly between $p = 0.09$ and $p = 0.20$, with values close to $k_F = 0.74$ Å^{-1} [45]. ARPES data on Hg1201 yield similar values of k_F and v_F [44].

A measurement of the zero-field thermal conductivity in the $T \to 0$ limit yields a residual linear term κ_0/T which is independent of disorder (i.e., universal) [19] and given only by the ratio v_F/v_Δ [20]. A prior measurement on YBCO $p = 0.18$ gave $\kappa_0/T = 0.16$ mW/K^{2}cm [46], in excellent agreement with the ARPES values for v_F and v_Δ in Bi2212, namely $v_F = 2.5 \times 10^5$ m/s and $v_\Delta = v_F/16$ [17,18], as discussed in [47]. We are therefore fully justified to use $k_F = 0.74$ Å^{-1} and $v_\Delta = 1.5 \times 10^4$ m/s in Eq. (8) for YBCO $p = 0.18$. Given the weak doping dependence of these two parameters (even in the presence of the pseudogap and charge order), we will also use the same values of k_F and v_F for Hg1223 ($p = 0.09, 0.10, 0.11$).

Equation (8) was used to extract $1/\ell_s$ from κ_{xy} for the three Hg1223 samples at $B = 0.5$ T (see Fig. 3), and the results are plotted in Fig. 5. The inverse thermal mean free path follows a cubic temperature dependence, consistent with the expected behavior of the scattering rate ($1/\tau_s = v_F/\ell_s$). A fit to the function $1/\ell_s = a + bT^3$ was performed for each sample, where the parameter a represents the elastic scattering of nodal quasiparticles on impurities, allowing the extraction of the residual mean free path ℓ_{s0} later in this work. The coefficient b characterizes the strength of inelastic scattering processes.

An intriguing feature in Fig. 5 is the significant difference in slopes between the three dopings, corresponding to variations in b. The extracted values of b are 79, 11, and 16 (in units of 1/m K^3) for Hg1223 samples with $p = 0.09$, $p = 0.10$, and $p = 0.11$, respectively. Theoretical studies have predicted a cubic temperature dependence of the nodal quasiparticle scattering rate in clean d-wave superconductors [22–25], with quasiparticle-quasiparticle interactions naturally giving rise to this behavior via Fermi's golden rule [22]. It has also been shown that scattering of nodal quasiparticles by spin fluctuations can lead to a T^3 dependence [23–25].

The extensive theoretical literature supporting spin-fluctuation scattering as the origin of the T^3 dependence,

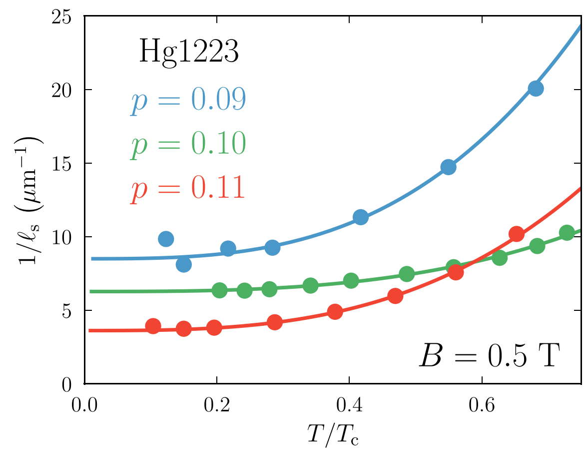

FIG. 5. Inverse mean free path $1/\ell_s$ as a function of temperature T for Hg1223 at 0.5 T: $p = 0.09$ (blue), $p = 0.10$ (green), and $p = 0.11$ (red). Markers represent the data points, while the lines correspond to T^3 fits ($a + bT^3$). The residual value at $T = 0$ is given by $\ell_{s0} = 1/a$, whose values are listed in Table I.

combined with the fact that the sample closest to the antiferromagnetic phase ($p = 0.09$) exhibits the highest b value, suggests that spin fluctuations could be the primary mechanism.

Rather than drawing a definitive conclusion, we present these results as a foundation for future investigations into the precise origin of the observed T^3 dependence.

For Hg1223, the residual mean free paths in the superconducting state are $\ell_{s0} = 1180 \pm 170$ Å, 1590 ± 230 Å, and 2760 ± 390 Å for $p = 0.09$, 0.10, and 0.11, respectively. These values of ℓ_{s0} correspond to $1/a$, where a is the parameter extracted from the cubic fit $1/\ell = a + bT^3$ applied to the data in Fig. 5 described earlier. These values are significantly higher than those typically observed in the normal state of clean cuprates such as Tl2201, where ℓ_{n0} is roughly 500 Å [48].

In Fig. 6, we compare the mean free path derived from Eq. (8) for data on Hg1223 $p = 0.11$ and data on YBCO $p = 0.18$, using the same k_F (0.74 Å^{-1}) and v_Δ (1.5×10^4 m/s). The comparable values of $\ell_{s0} = 2760 \pm 390$ Å for Hg1223 and $\ell_{s0} = 3530 \pm 500$ Å for YBCO highlight the exceptional cleanliness of Hg1223, as YBCO is the cleanest amongst cuprates. Furthermore, the value of $\ell_{s0} = 2760 \pm 390$ Å for Hg1223 at $p = 0.11$ is significantly higher than that of 1040 ± 150 Å for Hg1201. This suggests that the mean free path in the normal state of Hg1223 is likely much larger than the 200 Å reported for Hg1201 from the Dingle temperature of quantum oscillations [49]. This observation is consistent with reports of quantum oscillations in all three compounds (YBCO, Hg1201, and Hg1223) [49–53].

When comparing the mean free path of Hg1223 with that of the cleanest cuprate, fully oxygenated YBCO, the values are similar [see Fig. 6(a)]. However, the residual mean free path for Hg1223 represents a lower bound, as we assumed an equal contribution from all three layers. This assumption directly affects the value of the interplane separation d, which is taken as $d = 5.3$ Å when all three planes contribute. If only one plane contributes, the interplane separation increases to

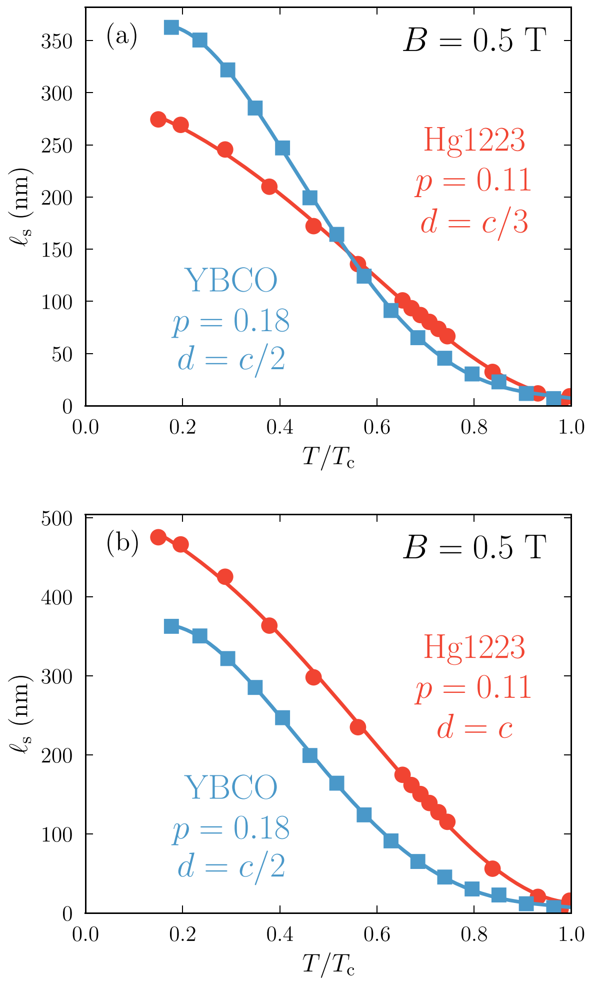

FIG. 6. Mean free path ℓ_s as a function of reduced temperature T/T_c for Hg1223 ($p = 0.11$, red, circle) and YBCO ($p = 0.18$, blue, square) at a magnetic field of 0.5 T. Markers represent the data points, and lines serve as guides to the eye. (a) Assuming that the three planes in Hg1223 contribute equally ($d = c/3$); (b) assuming that only the inner plane contributes ($d = c$).

$d = 16$ Å, leading to a higher calculated mean free path of $\ell_{s0} \approx 4600$ Å compared to $\ell_{s0} = 2760$ Å for $d = 5.3$ Å [see Fig. 6(b)] This suggests that the true mean free path of Hg1223 likely falls between these two extremes, indicating that its sample quality could exceed that of the cleanest YBCO. Hg1223, being the strongest cuprate superconductor, is also likely the cleanest.

To better understand the role of the outer layers in the sample quality of Hg1223, we compare its mean free path with that of its single-layered counterpart, Hg1201, both doped with $p = 0.10$. The comparison shows that trilayered Hg1223 exhibits significantly higher sample quality than single-layer Hg1201 (see Fig. 7). Once again, the estimated mean free path in Hg1223 represents a lower bound, highlighting the protective effect of the outer layers on the inner plane.

To validate the self-consistency of our framework, we verify the hypothesis $\omega_c\tau \ll 1$ for the YBCO sample, which has the highest residual mean free path, $\ell_{s0} = 3530$ Å. Using the expression $\omega_c\tau = eB\ell_{s0}/\hbar k_F$, we estimate $\omega_c\tau \sim 0.04$ at $B = 0.5$ T, confirming the self-consistency of our analysis.

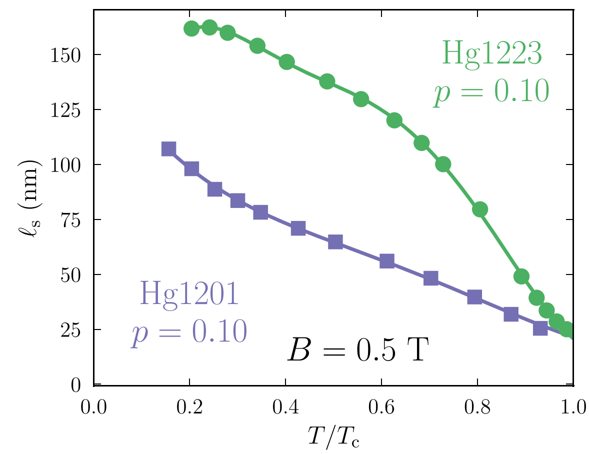

FIG. 7. Mean free path ℓ_s as a function of reduced temperature T/T_c for Hg1223 ($p = 0.10$, green, circle) and Hg1201 ($p = 0.10$, purple, square). Markers represent the data points, and lines serve as guides to the eye. From Eq. (8) using the same values of k_F and v_Δ, and assuming that the three planes in Hg1223 contribute equally ($d = c/3$).

C. Field dependence

The mean free path ℓ_s of nodal quasiparticles in the superconducting state depends on magnetic field, for two reasons. First, inelastic scattering grows with field, since the field excites quasiparticles and hence electron-electron scattering. Second, vortices can scatter heat carriers, including quasiparticles. This is why in clean samples the upper critical field H_{c2}—the field below which vortices form—can be detected by measuring the thermal conductivity: κ_{xx} drops sharply as H is reduced below H_{c2}, at $T \simeq 0$ [4]. In Fig. 8(a), we show the field dependence of ℓ_s in the five samples investigated here. The calculation uses the general, H- and T-dependent expression for the specific heat from Ref. [16]. [Note that using Eq. (8) instead makes little difference.] In two cases, Hg1223 $p = 0.10$ and Hg1201, a continuous field sweep was performed. In Hg1223 $p = 0.10$, ℓ_s exhibits a strong field dependence, increasing from 160 nm at $B = 0.5$ T to approximately 280 nm at $B \to 0$. A similarly strong H dependence is observed in Hg1223 $p = 0.11$ and YBCO. In contrast, Hg1201 shows a much weaker field dependence, with ℓ_s increasing only slightly from 70 nm at $B = 0.5$ T to 90 nm at $B \to 0$, comparable to what is seen in Hg1223 $p = 0.09$.

This field dependence implies that an estimate of ℓ_s should be taken in the $B \to 0$ limit. But comparing different samples or different cuprates, at a given finite field is nonetheless reasonable.

In Fig. 8(b), we reproduce the data of Zhang *et al.* both at $B = 0.5$ T and at $B \to 0$ [15]. We see that their data on YBCO $p = 0.18$ are in excellent quantitative agreement with ours, when both are taken at $B = 0.5$ T. We also see that the $T \to 0$ value is roughly twice as large at $B \to 0$.

V. CONCLUSION

We have measured the thermal Hall conductivity of three high-T_c cuprate superconductors, with a focus on the trilayer material Hg1223. From our data, we extract the quasiparticle

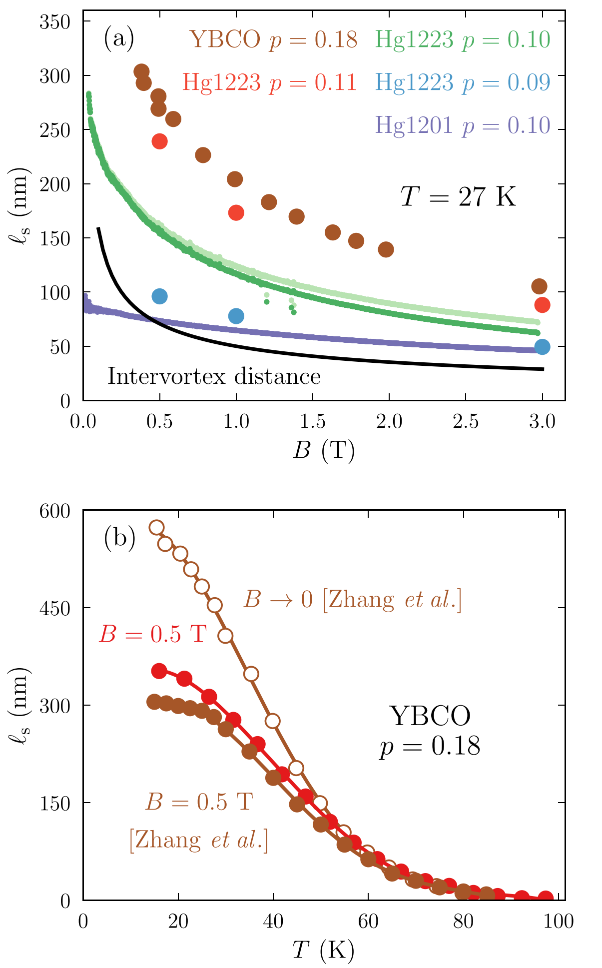

FIG. 8. (a) Mean free path ℓ_s as a function of magnetic field B at $T = 27$ K for YBCO ($p = 0.18$, brown), Hg1223 ($p = 0.09$, blue; $p = 0.10$, green; $p = 0.11$, red), and Hg1201 ($p = 0.10$, purple). The YBCO data at $B = 0.5$ T are taken from Fig. 2 of [15]. For Hg1201 ($p = 0.10$) and Hg1223 ($p = 0.10$), field sweeps of κ_{xy} were performed. For Hg1223 ($p = 0.09$) and ($p = 0.11$), ℓ_s was extracted from temperature step measurements of κ_{xy} at $B = 0.5$, 1, and 3 T (Fig. 1). The black line represents the intervortex distance, given by $50/\sqrt{B}$ nm [16]. The mean free path shown here is calculated using the general, H- and T-dependent expression for the specific heat from Ref. [16], except for the light green curve ($p = 0.10$) where Eq. (8) was used to illustrate the difference between the two approaches. (b) Mean free path ℓ_s as a function of temperature T for YBCO ($p = 0.18$). The red curve corresponds to ℓ_s extracted from our data at $B = 0.5$ T, while the brown curves represent the data from [15] at $B = 0.5$ T (full circles) and in the $B \to 0$ limit (open circles).

mean free path in the superconducting state via a simple model. By comparing the results with YBCO and Hg1201, we find that Hg1223 exhibits exceptional sample quality, potentially surpassing even the cleanest YBCO, the gold standard among cuprates. The trilayer structure of Hg1223 may play a crucial role, with the outer layers protecting the inner plane from disorder, resulting in a significantly higher mean free path compared to single-layer Hg1201. This suggests that the strongest cuprate superconductor, Hg1223, is also the cleanest.

We observe a cubic temperature dependence in the inverse mean free path, a behavior predicted for clean d-wave superconductors. More work is needed to understand how the strength of the inelastic scattering responsible for this T^3 dependence varies with doping.

ACKNOWLEDGMENTS

We thank Seyed Amirreza Ataei, Lu Chen, Robin Durand, Koko Mino, and Juan Vieira Giestinhas for fruitful discussions. We also thank Simon Fortier for his assistance with the experiments, and the cryogenics team at the Institut Quantique for their support. We are grateful to the Centre Tara for hosting a writing retreat that contributed to the completion of this manuscript. L.T. acknowledges support from the Canadian Institute for Advanced Research (CIFAR) as a CIFAR Fellow and funding from the Institut Quantique, the Natural Sciences and Engineering Research Council of Canada (Grant No. PIN:123817), the Canada Foundation for Innovation, and a Canada Research Chair. C.P. acknowledges support from the EUR grant NanoX No. ANR-17-EURE-0009 and from the ANR grant NEPTUN No. ANR-19-CE30-0019-01. G.G. acknowledges support from STeP2 No. ANR-22-EXES-0013, QuantExt No. ANR-23-CE30-0001-01, Audace CEA No. ANR-24-RRII-0004, and the École Polytechnique Foundation. M. Altangerel, Q. Barthélemy, É. Lefrançois, J. Baglo, M. Mezidi, A. Vallipuram, E. Campillo and L. Taillefer have benefitted from their affiliation to the RQMP [54]. This research was undertaken thanks, in part, to funding from the Canada First Research Excellence Fund. This research project No. 324046 is made possible thanks to funding from the Fonds de recherche du Québec.

DATA AVAILABILITY

The data that support the findings of this article are not publicly available. The data are available from the authors upon reasonable request.

[1] P. J. Hirschfeld and N. Goldenfeld, Effect of strong scattering on the low-temperature penetration depth of a d-wave superconductor, Phys. Rev. B **48**, 4219 (1993).
[2] M.-A. Park, M. H. Lee, and Y.-J. Kim, Impurity scattering in a d-wave superconductor, Mod. Phys. Lett. B **11**, 719 (1997).
[3] Y. Sun and K. Maki, Impurity effects in d-wave superconductors, Phys. Rev. B **51**, 6059 (1995).
[4] G. Grissonnanche, O. Cyr-Choinière, F. Laliberté, S. René De Cotret, A. Juneau-Fecteau, S. Dufour-Beauséjour, M. E. Delage, D. LeBoeuf, J. Chang, B. J. Ramshaw, D. A. Bonn, W. N. Hardy, R. Liang, S. Adachi, N. E. Hussey, B. Vignolle, C. Proust, M. Sutherland, S. Krämer, J. H. Park *et al.*, Direct measurement of the upper critical field in cuprate superconductors, Nat. Commun. **5**, 3280 (2014).
[5] C. Proust, E. Boaknin, R. W. Hill, L. Taillefer, and A. P. Mackenzie, Heat transport in a strongly overdoped cuprate: Fermi liquid and a pure d-wave BCS superconductor, Phys. Rev. Lett. **89**, 147003 (2002).

[6] A. Legros, S. Benhabib, W. Tabis, F. Laliberté, M. Dion, M. Lizaire, B. Vignolle, D. Vignolles, H. Raffy, Z. Z. Li, P. Auban-Senzier, N. Doiron-Leyraud, P. Fournier, D. Colson, L. Taillefer, and C. Proust, Universal T-linear resistivity and Planckian dissipation in overdoped cuprates, Nat. Phys. **15**, 142 (2019).

[7] R. A. Cooper, Y. Wang, B. Vignolle, O. J. Lipscombe, S. M. Hayden, Y. Tanabe, T. Adachi, Y. Koike, M. Nohara, H. Takagi, C. Proust, and N. E. Hussey, Anomalous criticality in the electrical resistivity of $YBa_2Cu_3O_7$, Science **323**, 603 (2009).

[8] A. Ataei, A. Gourgout, G. Grissonnanche, L. Chen, J. Baglo, M.-E. Boulanger, F. Laliberté, S. Badoux, N. Doiron-Leyraud, V. Oliviero, S. Benhabib, D. Vignolles, J.-S. Zhou, S. Ono, H. Takagi, C. Proust, and L. Taillefer, Electrons with Planckian scattering obey standard orbital motion in a magnetic field, Nat. Phys. **18**, 1420 (2022).

[9] R. Daou, O. Cyr-Choinière, F. Laliberté, D. LeBoeuf, N. Doiron-Leyraud, J.-Q. Yan, J.-S. Zhou, J. B. Goodenough, and L. Taillefer, Thermopower across the stripe critical point of $La_{1.6-x}Nd_{0.4}Sr_xCuO_4$: Evidence for a quantum critical point in a hole-doped high-T_c superconductor, Phys. Rev. B **79**, 180505 (2009).

[10] C. Collignon, S. Badoux, S. A. A. Afshar, B. Michon, F. Laliberté, O. Cyr-Choinière, J.-S. Zhou, S. Licciardello, S. Wiedmann, N. Doiron-Leyraud, and L. Taillefer, Fermi-surface transformation across the pseudogap critical point of the cuprate superconductor $La_{1.6-x}Nd_{0.4}Sr_xCuO_4$, Phys. Rev. B **95**, 224517 (2017).

[11] F. Laliberté, W. Tabis, S. Badoux, B. Vignolle, D. Destraz, N. Momono, T. Kurosawa, K. Yamada, H. Takagi, N. Doiron-Leyraud, C. Proust, and L. Taillefer, Origin of the metal-to-insulator crossover in cuprate superconductors, arXiv:1606.04491.

[12] C. Proust and L. Taillefer, The remarkable underlying ground states of cuprate superconductors, Annu. Rev. Condens. Matter Phys. **10**, 409 (2019).

[13] M. Frachet, I. Vinograd, R. Zhou, S. Benhabib, S. Wu, H. Mayaffre, S. Krämer, S. K. Ramakrishna, A. P. Reyes, J. Debray, T. Kurosawa, N. Momono, M. Oda, S. Komiya, S. Ono, M. Horio, J. Chang, C. Proust, D. LeBoeuf, and M.-H. Julien, Hidden magnetism at the pseudogap critical point of a cuprate superconductor, Nat. Phys. **16**, 1064 (2020).

[14] D. J. Campbell, M. Frachet, V. Oliviero, T. Kurosawa, N. Momono, M. Oda, J. Chang, D. Vignolles, C. Proust, and D. LeBoeuf, Strange metal from spin fluctuations in a cuprate superconductor, arXiv:2412.0372.

[15] Y. Zhang, N. P. Ong, P. W. Anderson, D. A. Bonn, R. Liang, and W. N. Hardy, Giant enhancement of the thermal Hall conductivity κ_{xy} in the superconductor $YBa_2Cu_3O_7$, Phys. Rev. Lett. **86**, 890 (2001).

[16] I. Vekhter, P. J. Hirschfeld, and E. J. Nicol, Thermodynamics of d-wave superconductors in a magnetic field, Phys. Rev. B **64**, 064513 (2001).

[17] I. M. Vishik, W. S. Lee, F. Schmitt, B. Moritz, T. Sasagawa, S. Uchida, K. Fujita, S. Ishida, C. Zhang, T. P. Devereaux, and Z. X. Shen, Doping-dependent nodal Fermi velocity of the high-temperature superconductor $Bi_2Sr_2CaCu_2O_{8+\delta}$ revealed using high-resolution angle-resolved photoemission spectroscopy, Phys. Rev. Lett. **104**, 207002 (2010).

[18] I. M. Vishik, M. Hashimoto, R.-H. He, W.-S. Lee, F. Schmitt, D. Lu, R. G. Moore, C. Zhang, W. Meevasana, T. Sasagawa, S. Uchida, K. Fujita, S. Ishida, M. Ishikado, Y. Yoshida, H. Eisaki, Z. Hussain, T. P. Devereaux, and Z.-X. Shen, Phase competition in trisected superconducting dome, Proc. Natl. Acad. Sci. USA **109**, 18332 (2012).

[19] L. Taillefer, B. Lussier, R. Gagnon, K. Behnia, and H. Aubin, Universal heat conduction in $YBa_2Cu_3O_{6.9}$, Phys. Rev. Lett. **79**, 483 (1997).

[20] A. C. Durst and P. A. Lee, Impurity-induced quasiparticle transport and universal-limit Wiedemann-Franz violation in d-wave superconductors, Phys. Rev. B **62**, 1270 (2000).

[21] M. Sutherland, D. G. Hawthorn, R. W. Hill, F. Ronning, S. Wakimoto, H. Zhang, C. Proust, E. Boaknin, C. Lupien, L. Taillefer, R. Liang, D. A. Bonn, W. N. Hardy, R. Gagnon, N. E. Hussey, T. Kimura, M. Nohara, and H. Takagi, Thermal conductivity across the phase diagram of cuprates: Low-energy quasiparticles and doping dependence of the superconducting gap, Phys. Rev. B **67**, 174520 (2003).

[22] M. B. Walker and M. F. Smith, Quasiparticle-quasiparticle scattering in high-T_c superconductors, Phys. Rev. B **61**, 11285 (2000).

[23] T. Dahm, P. J. Hirschfeld, D. J. Scalapino, and L. Zhu, Nodal quasiparticle lifetimes in cuprate superconductors, Phys. Rev. B **72**, 214512 (2005).

[24] D. Duffy, P. J. Hirschfeld, and D. J. Scalapino, Quasiparticle lifetimes in a $d_{x^2-y^2}$ superconductor, Phys. Rev. B **64**, 224522 (2001).

[25] S. M. Quinlan, D. J. Scalapino, and N. Bulut, Superconducting quasiparticle lifetimes due to spin-fluctuation scattering, Phys. Rev. B **49**, 1470 (1994).

[26] B. Loret, A. Forget, J.-B. Moussy, S. Poissonnet, P. Bonnaillie, G. Collin, P. Thuery, A. Sacuto, and D. Colson, Crystal growth and characterization of $HgBa_2Ca_2Cu_3O_{8+\delta}$ superconductors with the highest critical temperature at ambient pressure, Inorg. Chem. **56**, 9396 (2017).

[27] M. Presland, J. Tallon, R. Buckley, R. Liu, and N. Flower, General trends in oxygen stoichiometry effects on T_c in Bi and Tl superconductors, Physica C: Supercond. **176**, 95 (1991).

[28] N. Barišić, Y. Li, X. Zhao, Y.-C. Cho, G. Chabot-Couture, G. Yu, and M. Greven, Demonstrating the model nature of the high-temperature superconductor $HgBa_2CuO_{4+\delta}$, Phys. Rev. B **78**, 054518 (2008).

[29] X. Zhao, G. Yu, Y.-C. Cho, G. Chabot-Couture, N. Barišić, P. Bourges, N. Kaneko, Y. Li, L. Lu, E. M. Motoyama *et al.*, Crystal growth and characterization of the model high-temperature superconductor $HgBa_2CuO_{4+\delta}$, Adv. Mater. **18**, 3243 (2006).

[30] A. Yamamoto, W.-Z. Hu, and S. Tajima, Thermoelectric power and resistivity of $HgBa_2CuO_{4+\delta}$ over a wide doping range, Phys. Rev. B **63**, 024504 (2000).

[31] R. Liang, D. A. Bonn, and W. N. Hardy, Evaluation of CuO_2 plane hole doping in $YBa_2Cu_3O_{6+x}$ single crystals, Phys. Rev. B **73**, 180505 (2006).

[32] G. Grissonnanche, F. Laliberté, S. Dufour-Beauséjour, M. Matusiak, S. Badoux, F. F. Tafti, B. Michon, A. Riopel, O. Cyr-Choinière, J. C. Baglo, B. J. Ramshaw, R. Liang, D. A. Bonn, W. N. Hardy, S. Krämer, D. LeBoeuf, D. Graf, N. Doiron-Leyraud, and L. Taillefer, Wiedemann-franz law in the underdoped cuprate superconductor $YBa_2Cu_3O_y$, Phys. Rev. B **93**, 064513 (2016).

[33] G. Grissonnanche, S. Thériault, A. Gourgout, M.-E. Boulanger, E. Lefrançois, A. Ataei, F. Laliberté, M. Dion, J.-S. Zhou, S. Pyon, T. Takayama, H. Takagi, N. Doiron-Leyraud, and L. Taillefer, Chiral phonons in the pseudogap phase of cuprates, Nat. Phys. **16**, 1108 (2020).
[34] A. Vallipuram, L. Chen, E. Campillo, M. Mezidi, G. Grissonnanche, M.-E. Boulanger, E. Lefrançois, M. P. Zic, Y. Li, I. R. Fisher, J. Baglo, and L. Taillefer, Role of magnetic ions in the thermal Hall effect of the paramagnetic insulator $TmVO_4$, Phys. Rev. B **110**, 045144 (2024).
[35] L. Chen, E. Lefrançois, A. Vallipuram, Q. Barthélemy, A. Ataei, W. Yao, Y. Li, and L. Taillefer, Planar thermal Hall effect from phonons in a Kitaev candidate material, Nat. Commun. **15**, 3513 (2024).
[36] E. Lefrançois, G. Grissonnanche, J. Baglo, P. Lampen-Kelley, J.-Q. Yan, C. Balz, D. Mandrus, S. E. Nagler, S. Kim, Y.-J. Kim, N. Doiron-Leyraud, and L. Taillefer, Evidence of a phonon Hall effect in the Kitaev spin liquid candidate α-$RuCl_3$, Phys. Rev. X **12**, 021025 (2022).
[37] M.-E. Boulanger, G. Grissonnanche, S. Badoux, A. Allaire, E. Lefrançois, A. Legros, A. Gourgout, M. Dion, C. H. Wang, X. H. Chen, R. Liang, W. N. Hardy, D. A. Bonn, and L. Taillefer, Thermal Hall conductivity in the cuprate Mott insulators Nd_2CuO_4 and $Sr_2CuO_2Cl_2$, Nat. Commun. **11**, 5325 (2020).
[38] P. J. Hirschfeld and W. O. Putikka, Theory of thermal conductivity in $YBa_2Cu_3O_{7-\delta}$, Phys. Rev. Lett. **77**, 3909 (1996).
[39] M. Lizaire, A. Legros, A. Gourgout, S. Benhabib, S. Badoux, F. Laliberté, M.-E. Boulanger, A. Ataei, G. Grissonnanche, D. LeBoeuf, S. Licciardello, S. Wiedmann, S. Ono, H. Raffy, S. Kawasaki, G.-Q. Zheng, N. Doiron-Leyraud, C. Proust, and L. Taillefer, Transport signatures of the pseudogap critical point in the cuprate superconductor $Bi_2Sr_{2-x}La_xCuO_6+\delta$, Phys. Rev. B **104**, 014515 (2021).
[40] M.-E. Boulanger, G. Grissonnanche, E. Lefrançois, A. Gourgout, K.-J. Xu, Z.-X. Shen, R. L. Greene, and L. Taillefer, Thermal Hall conductivity of electron-doped cuprates, Phys. Rev. B **105**, 115101 (2022).
[41] M.-E. Boulanger, L. Chen, V. Oliviero, D. Vignolles, G. Grissonnanche, K. Xu, Z.-X. Shen, C. Proust, J. Baglo, and L. Taillefer, Thermal Hall conductivity of electron-doped cuprates: Electrons and phonons, arXiv:2310.15892.
[42] G. Grissonnanche, A. Legros, S. Badoux, E. Lefrançois, V. Zatko, M. Lizaire, F. Laliberté, A. Gourgout, J.-S. Zhou, S. Pyon, T. Takayama, H. Takagi, S. Ono, N. Doiron-Leyraud, and L. Taillefer, Giant thermal Hall conductivity in the pseudogap phase of cuprate superconductors, Nature (London) **571**, 376 (2019).
[43] D. A. Wright, J. P. Emerson, B. F. Woodfield, J. E. Gordon, R. A. Fisher, and N. E. Phillips, Low-temperature specific heat of $YBa_2Cu_3O_{7-\delta}$, $0 \leqslant \delta \leqslant 0.2$: Evidence for d-wave pairing, Phys. Rev. Lett. **82**, 1550 (1999).
[44] I. M. Vishik, N. Barišić, M. K. Chan, Y. Li, D. D. Xia, G. Yu, X. Zhao, W. S. Lee, W. Meevasana, T. P. Devereaux, M. Greven, and Z.-X. Shen, Angle-resolved photoemission spectroscopy study of $HgBa_2CuO_{4+\delta}$, Phys. Rev. B **89**, 195141 (2014).
[45] K. Fujita, C. K. Kim, I. Lee, J. Lee, M. H. Hamidian, I. A. Firmo, S. Mukhopadhyay, H. Eisaki, S. Uchida, M. J. Lawler, E.-A. Kim, and J. C. Davis, Simultaneous transitions in cuprate momentum-space topology and electronic symmetry breaking, Science **344**, 612 (2014).
[46] R. W. Hill, C. Lupien, M. Sutherland, E. Boaknin, D. G. Hawthorn, C. Proust, F. Ronning, L. Taillefer, R. Liang, D. A. Bonn, and W. N. Hardy, Transport in ultraclean $YBa_2Cu_3O_7$: Neither unitary nor Born impurity scattering, Phys. Rev. Lett. **92**, 027001 (2004).
[47] J.-P. Reid, A. Juneau-Fecteau, R. T. Gordon, S. René de Cotret, N. Doiron-Leyraud, X. G. Luo, H. Shakeripour, J. Chang, M. A. Tanatar, H. Kim, R. Prozorov, T. Saito, H. Fukazawa, Y. Kohori, K. Kihou, C. H. Lee, A. Iyo, H. Eisaki, B. Shen, H.-H. Wen *et al.*, From d-wave to s-wave pairing in the iron-pnictide superconductor (Ba,K)Fe_2As_2, Supercond. Sci. Technol. **25**, 084013 (2012).
[48] A. P. Mackenzie, S. R. Julian, D. C. Sinclair, and C. T. Lin, Normal-state magnetotransport in superconducting $Tl_2Ba_2CuO_{6+\delta}$ to millikelvin temperatures, Phys. Rev. B **53**, 5848 (1996).
[49] M. K. Chan, N. Harrison, R. D. McDonald, B. J. Ramshaw, K. A. Modic, N. Barišić, and M. Greven, Single reconstructed Fermi surface pocket in an underdoped single-layer cuprate superconductor, Nat. Commun. **7**, 12244 (2016).
[50] V. Oliviero, S. Benhabib, I. Gilmutdinov, B. Vignolle, L. Drigo, M. Massoudzadegan, M. Leroux, G. L. J. A. Rikken, A. Forget, D. Colson, D. Vignolles, and C. Proust, Magnetotransport signatures of antiferromagnetism coexisting with charge order in the trilayer cuprate $HgBa_2Ca_2Cu_3O_{8+\delta}$, Nat. Commun. **13**, 1568 (2022).
[51] V. Oliviero, I. Gilmutdinov, D. Vignolles, S. Benhabib, N. Bruyant, A. Forget, D. Colson, W. A. Atkinson, and C. Proust, Charge order near the antiferromagnetic quantum critical point in the trilayer high T_c cuprate $HgBa_2Ca_2Cu_3O_{8+\delta}$, npj Quantum Mater. **9**, 75 (2024).
[52] N. Barišić, S. Badoux, M. K. Chan, C. Dorow, W. Tabis, B. Vignolle, G. Yu, J. Béard, X. Zhao, C. Proust, and M. Greven, Universal quantum oscillations in the underdoped cuprate superconductors, Nat. Phys. **9**, 761 (2013).
[53] N. Doiron-Leyraud, C. Proust, D. LeBoeuf, J. Levallois, J.-B. Bonnemaison, R. Liang, D. A. Bonn, W. N. Hardy, and L. Taillefer, Quantum oscillations and the fermi surface in an underdoped high-T_c superconductor, Nature (London) **447**, 565 (2007).
[54] https://doi.org/10.69777/309032.